OPEN ACCESS

GAVIN PUBLISHERS

Nanomedicine and Nanoscience Research

Research Article

Mayedwa N, et al. J Nanomed Nanosci: JNAN-150.

DOI: 10.29011/2577-1477.100050

Development of a Novel Tyrosinase Amperometric Biosensor Based on Tin Nanoparticles for the Detection of Bisphenol A (4.4-Isopropylidene-diphenol) in Water

Noluthando Mayedwa[1,2*], Aline Simo[2], Itani Given Madiba[1,2], Lisebo Phelane[3], Rachel Fanelwa Ajayi[3], Nolubabalo Matinise[2], Nametso Mongwaketsi[2], Malik Maaza[1,2]

[1]College of Graduate Studies, University of South Africa, UNESCO-Africa Chair in Nanoscience and Nanotechnology, Theo Van Wyk Building, UNISA, South Africa

[2]Material Research Department, iThemba Laboratory for Accelerator Based Science, Somerset West, South Africa

[3]University of the Western Cape, Chemical Science Building, Sensor LAB, Private Bag, Bellville, South Africa

[*]**Corresponding author:** Noluthando Mayedwa, College of Graduate Studies, University of South Africa, UNESCO-Africa Chair in Nanoscience and Nanotechnology, Theo Van Wyk Building 9-119, P. O Box 392, UNISA 0003, South Africa. Tel: +27218431000; Email: nmayedwa@tlabs.ac.za

Citation: Mayedwa N, Simo A, Madiba IG, Phelane L, Ajayi AF, et al. (2018) Development of a Novel Tyrosinase Amperometric Biosensor Based on Tin Nanoparticles for the Detection of Bisphenol A (4.4-Isopropylidenediphenol) in Water. J Nanomed Nanosci: JNAN-150. DOI: 10.29011/2577-1477.100050

Received Date: 30 July, 2018; **Accepted Date:** 08 August, 2018; **Published Date:** 14 August, 2018

Abstract

Highly crystalline Poly-Vinyl Pyrrolidone (PVP) capped Sn (Tin) Nanoparticles (NP) with good size and shape uniformity was synthesized by a hydrothermal process. A highly sensitive amperometric biosensor for the detection of bisphenol A (BPA) was developed by immobilizing tyrosinase on to Glassy Carbon Electrode (GCE) modified with Sn nanoparticles. The fabricated amperometric biosensor exhibited excellent electroactivity towards BPA oxidation catalysed by enzymatic reaction of tyrosinase together with good conductivity of Sn nanoparticles. The developed biosensor displayed linear range from 0.01 to 0.10 µmol L-1 and a Detection Limit (DL) of 1.8 nmol L-1 with a correlation coefficient of 0.989. Electrochemical Impedance Spectroscopy (EIS) obtained in buffer solution for tyrosinase/SnNP/ GCE had the lowest charge transfer resistance (Rct) value of 219 Ω, which indicated low charge transfer. There was an increase in Rct for tyrosinase/GCE, SnNP/GCE and Bare GCE which was 316 Ω, 638 Ω and 598 Ω respectively. This indicated a strong resistance to charge transfer. The bode plot showed a phase angle values for tyrosinase/SnNP/GCE, tyrosinase/GCE, SnNP/GCE and Bare GCE was 81º, 61º, 74º and 59º respectively, showed semiconductor behavior due to the presence of Sn nanoparticles and tyrosinase catalytic abilities. It is reported for the first time the use of Sn nanoparticles modified on GCE and tyrosinase for detection of BPA.

Keywords: Biosensor; Bisphenol A; Electrochemistry; Nanoparticles, Tyrosinase

Introduction

Recently, environmental pollution by endocrine disrupting compounds has attracted increased attention [1]. Phenols, bisphenol A, dyes, pharmaceuticals, parabens, are endocrine disrupting compounds and are all severe environmental pollutants that are introduced into the environment from chemical and pharmaceutical industries [2,3]. Bisphenol A (BPA, 2, 2-bis (4-hydroxyphenyl) propane) is widely used as a monomer in the production of epoxy resins and polycarbonate plastics. These plastics are used in much food and drink packaging applications, whilst the resins are commonly used as lacquers to coat metal products such as food cans, bottle tops and water supply pipes [4-6]. Endocrine disrupting compounds do not degrade easily in the environment [4,7]. It can accumulate in living tissue which act as an estrogens and may lead to negative health effects, thereby, disrupting the normal function of the endocrine system [7].

Prolonged exposure and absorption of bisphenol A can also lead to death [6]. To date, internationally standardized methods to detect these substances have not been agreed upon [6-7]. In addition, the most common analytical technique for endocrine disrupting compounds detection is Mass Spectrometric

(MS) analysis, High Performance Liquid Chromatography (HPLC), Liquid Chromatography Tandem Mass Spectrometry (LC-MS-MS) and Gas Chromatography Coupled with Mass Spectrometry (GC-MS) [3,8,9]. However, it is well known that the instrumentation is expensive and requires time consuming extraction or pre concentration steps in addition to skilled operators [10,11]. Electrochemical methods have shown great potential for environmental monitoring because of its advantages such as easy to handle due to small size, fast response speed, low cost, timesaving, high sensitivity, excellent selectivity, and in vivo real-time determination [8,10,12]. However, a major obstacle encountered in the detection of BPA by electrochemical method is the relatively high over potential together with poor reproducibility although BPA can be oxidized at electrode surface due to containing phenol hydroxyl group [13].

Bare electrode often suffers from a fouling effect, which causes rather poor selectivity and sensitivity. An effective way to overcome electrode fouling is by electrode modification, of which is capable of improving electrochemical activity by overcoming the slow kinetics of many electrode processes [12-14]. The electrode is usually modified with enzymes, polymers, and nanoparticles [13]. Sn nanoparticles are synthesized and modified on glassy carbon electrode, owning to their high electrical catalytic properties, high chemical stability and extremely high mechanical strength [15]. Due to the potential application in diverse fields, metal nanoparticles have attracted great attention in recent years [16,17]. These ultra-fine particles often exhibit unusual physical and chemical properties that are distinct from either simple molecules or bulk materials. Current research in this area is motivated by the possible application of these unique properties [15,18,19].

Here we described a new tyrosinase biosensor based on the immobilization of tyrosinase with Bovine Serum Albumin (BSA) which prevents adhesion of enzyme to the electrode surface on to the Sn nanoparticles on the glassy carbon electrode. The modified glassy carbon electrode was used for the detection of BPA in 0.1 M phosphate buffer solution (pH 7), glutaraldehyde was used as a cross linker for detection of BPA. Components of Sn nanoparticles before modification were characterized by High Resolution Scanning Electrode Microscopy (HRSEM), High Resolution Transmission Electron Microscopy (HRTEM), X-ray Diffraction (XRD) and Fourier Transmission Infrared Spectroscopy (FTIR). The response dependences and amperometric characteristics of the prepared enzyme electrode in the detection of BPA compounds was investigated. The results showed that the developed biosensor exhibited good stability and high sensitivity for the detection of BPA compounds.

Experimental Details

Reagents and Materials

Phosphate Buffer Solution (PBS) at pH 7.0 was prepared by mixing NaH_2PO_4 and Na_2HPO_4 then adjusted pH with NaOH. Glutaraldehyde solution (50 wt. % in H_2O, $OHC(CH_2)_3CHO$), Bovine Serum Albumin (BSA), Tyrosinase from mushroom, Bisphenol A (2,2-Bis(4-hydroxyphenyl) propane, $(CH_3)_2C(C_6H_4OH)_2$), Polyvinyl pyrrolidone (PVP, MW = 55000), Sodium borohydride ($NaBH_4$), Tin (II) chloride dehydrate ($SnCl_2.2H_2O$), Potassium chloride (KCl), Potassium ferrocyanide ($K_4[Fe(CN)_6]3H_2O$) and absolute ethanol (CH_3CH_2OH) were all purchased from Sigma-Aldrich. Alumina micro powder and polishing pads were obtained from Buehler, IL, USA and were used for polishing the Glassy Carbon Electrode (GCE) electrodes. Ultra-pure water (Millipore) was used in the preparation of the aqueous solutions.

Instrumentation

All voltammetric measurements were performed on a BAS 100W electrochemical workstation from BioAnalytical Systems Incorporation (Lafayette, USA) using a 20 mL electrochemical cell with a conventional three-electrode system consisting of GCE (0.071 cm^2 diameter) working electrode, Ag/AgCl (saturated NaCl) reference electrode and platinum wire as counter electrode. Cyclic voltammetry (CV) were recorded with a computer interfaced to the machine. All experimental solutions were purged and blanketed with a highly purified argon gas. The experiments were carried out at controlled room temperature (25°C). Electrochemical Impedance Spectroscopy (EIS) was recorded with Zahner IM6ex Germany at perturbation amplitude of 10 mV within the frequency range of 100 kHz and 100 MHz. X-ray Diffraction (XRD) analysis of Sn nanoparticles solid catalytic samples were mounted upon in plastic sample holders and the surface was flattened to allow maximum X-ray exposure. The measurements were done in X-ray Diffractometer: Bruker AXS D8 Advance. High resolution transmission electron microscopy (HRTEM), images of Selected Area Electron Diffraction Pattern (SEAD) and Energy-Dispersive X-Rays (EDX) spectra were acquired using a Tecnai $G^2 F_2O$ X-Twin MAT. The HRTEM characterizations were performed by placing a drop of the solution on a carbon coated copper and nickel grid and dried under electric bulb for 15 min. High Resolution Scanning Electron Microscopy (HRSEM), Specimens had to be coated with carbon in order to be used in an HRSEM. Hitachi X-650 SEM.

Preparation of Tyrosinase on Glassy Carbon Electrode

0.1 % tyrosinase solution and 2 % bovine serum albumin solution was prepared in buffer solution (0.1 M, PBS pH 7).

Tyrosinase and BSA solutions were mixed together, prepared 2.5 % Glutaraldehyde solution in ultra-pure water. 2:1 solution mixture of tyrosinase + BSA: Glutaraldehyde solution was prepared and drop coated 10 µL of the solution on glassy carbon electrode.

Chemical Synthesis of Sn Nanoparticles

Typical synthesis consists of dissolving $SnCl_2.2H_2O$ and PVP in 30 mL deionised water distilled under constant stirring, a slurry white precipitate was formed in solution. $NaBH_4$ solution was prepared in 10 mL distilled water kept in ice and it was introduced to the reaction mixture drop wise over 30 minutes. After stirring, the solution was then transferred to a Teflon lined stainless steel autoclave, which was maintained at 160°C for 24 hours and cooled at room temperature. The product was centrifuged and washed several times with deionised water and absolute ethanol to remove impurities, the final product was dried at 90°C for 120 min.

Electrochemistry

Voltammetric and amperometric measurements were carried out with a potentiostat / galvanostat in 20 mL electrochemical cell with a conventional three-electrode system consisting of GCE (0.071 cm^2 diameter) working electrode, Ag/AgCl (saturated NaCl) reference electrode and platinum wire as counter electrode. The prepared tyrosinase was drop coated on glassy carbon electrode and was used as a working electrode to study its electrochemical activity. Cyclic Voltammetry (CV) was typically performed at a scan rate of 50 mV s^{-1} over a potential window of 0.3 to 0.8 V unless otherwise stated; all experiments were carried out at room temperature in Phosphate Buffer Solution (PBS) (0.1 M, pH 7). The schematic representation on how the biosensor is constructed is shown in Figure 1.

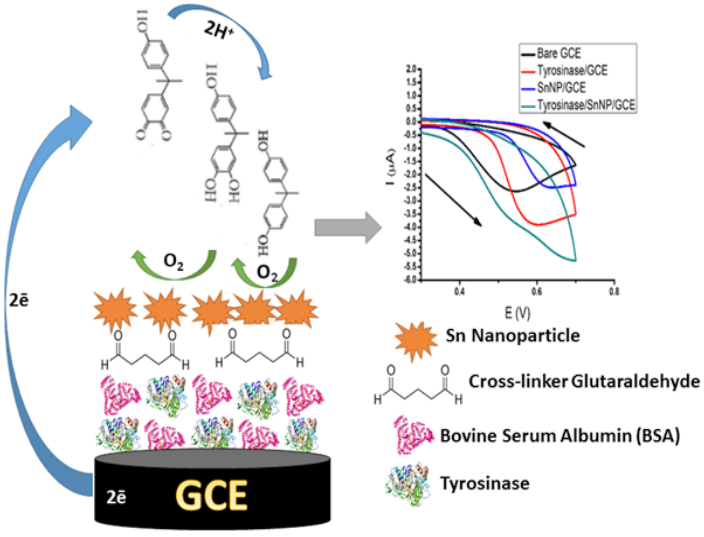

Figure 1: Schematic illustration of functionalizing procedure and Tyrosinase/Sn nanoparticles attachment on the GCE surface.

Results and Discussion

Characterization

The XRD patterns for the dried Sn NPs are shown in Figure 2. the diffraction peaks at 30.4°, 31.9°, 43.7°, 44.8°, 51.5°, 55.3°, 62.5°, 64.8°, 72.4°, 79.5° and 84.3° positions can be well-assigned to (200), (101), (220), (211), (301), (112), (400), (321), (420), (411) and (312) planes of Sn with tetragonal structure. While the diffraction peaks were broadened because the powders were nanosized, many peaks, including the main peak corresponding to (211) reflections, can be clearly observed. The average size of the Sn NPs was estimated from the average full width at half maximum of the (211) peak, according to Scherrer's equation [20,21]. The value obtained was ~3.29 nm, PVP coating on Sn NPs prevented the aggregation of Sn NPs, and the synergistic effect between core Sn NPs and PVP shell effectively alleviates the crystal grain growth, leading to smaller crystal size Sn NPs [22].

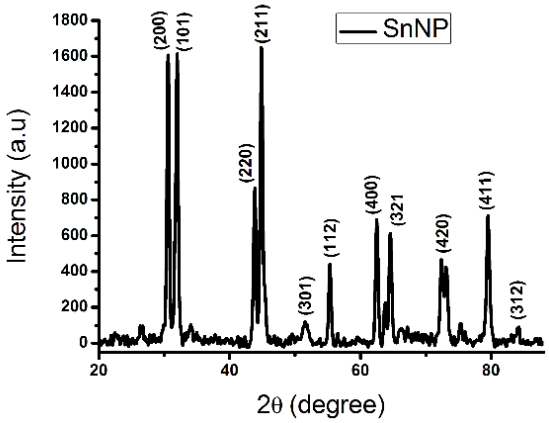

Figure 2: XRD pattern of hydrothermal Sn nanoparticles capped with PVP.

Figure 3(a) shows the HRTEM images of the synthesized Sn NPs capped with PVP. The nanoparticles were agglomerated and exhibited spherical and slightly elongated morphologies. The size of Sn NPs is about 5 to 13 nm; most of the particles have a diameter of 2 to 5 nm indicating a narrow size distribution. PVP coating on the surface of Sn NPs can effectively confine the Sn NPs within the PVP shell preventing aggregation. Figure 3(b) shows d-spacing of 0.28 Å corresponding well to (211) plane of tetragonal Sn nanoparticles, which further confirms the presence of crystalline Sn nanoparticles [19]. In Figure 3(c) shows polycrystalline rings in the Selected Area Electron Diffraction (SAED) pattern. This further confirmed the presence of β-Sn. The clear ring fringes indicated that crystallization occurred along different growth planes in a group of NPs or in an individual NP. The interplanar distance was measured corresponded to the interplanar distance between the (211) planes of β-Sn of the narrow size distribution of

the NPs. To investigate the elemental composition of the prepared Sn NPs, EDX was used in Figure 3(d). The elemental signals were oxygen, nickel, copper and tin. The presence of oxygen is due to the presence of PVP in the NPs while nickel and copper is as a result of the grid used to drop coat NPs for HRTEM analysis.

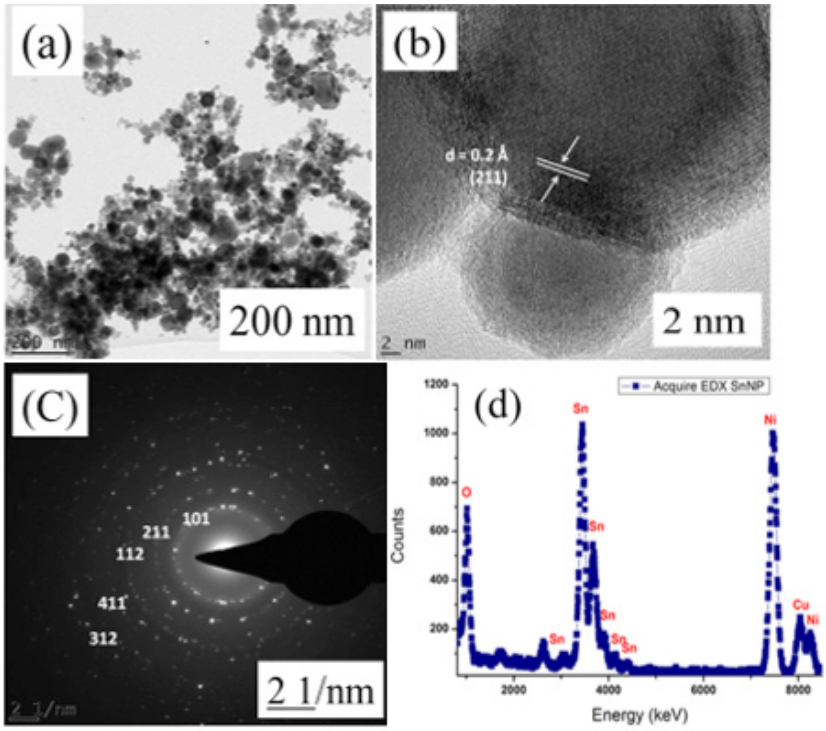

Figures 3(a-d): TEM images Sn NPs capped with PVP **(a)** Low-magnification TEM image. **(b)** High resolution TEM image. **(c)** Selected Area Electron Diffraction Pattern (SAED). **(d)** Energy Dispersive X ray (EDX) spectrum.

The High Resolution Scanning Electron Microscope (HRSEM) provided further insight into the morphology and size details of the Sn NPs capped with PVP. The HRSEM images of prepared sample are shown in given Figure 4(a). It can be seen that Sn nanoparticles possess uniform grains and is almost homogeneously distributed, which indicates the high packing density of these particles. In Figure 4(b) insert shows highly packed density of these nanoparticles, it can be understood easily that the as prepared Sn particles are fine and some agglomeration of finer particulates to form bigger clusters existed. Particle size and distribution of nanoparticles mainly depend upon the relative rates of nucleation and growth processes, as well as the extent of agglomeration [23].

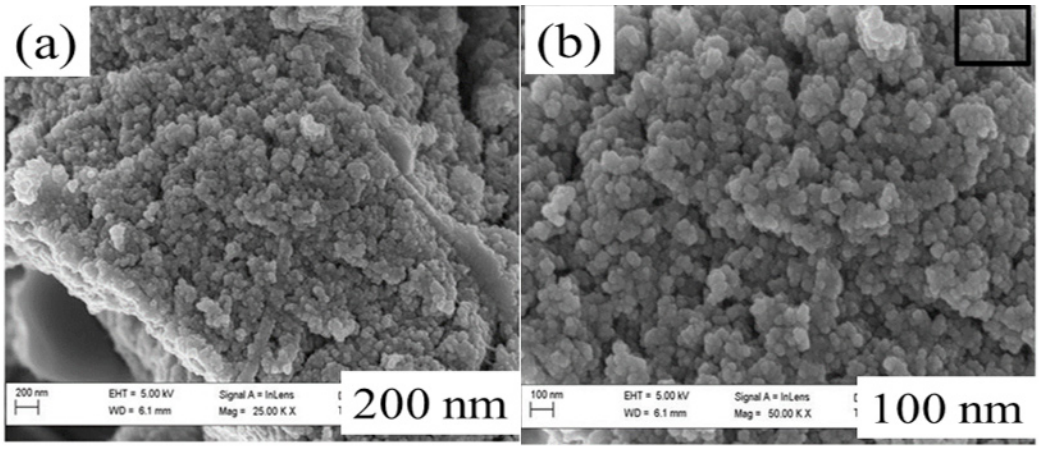

Figures 4 (a, b): (a) HRSEM images of Sn nanoparticles capped with PVP. **(b)** The insert shows packed density of nanoparticles.

In order to further describe the chemical composition component of the Sn NPs capped with PVP Fourier Transform Infrared Spectroscopy (FTIR) characterization was carried out in Figure 5. The FTIR spectrum of PVP capped Sn NPs presents the O-H group (3016 cm^{-1}), methylene asymmetric and symmetric C-H stretching (2412 cm^{-1} and 2258cm^{-1}), C=O stretching vibration (1666 cm^{-1}), CH_2 bending vibration (1306 cm^{-1}), C-N stretching vibration band (1094 cm^{-1}) and Sn-OH stretching vibration band (541 cm^{-1}) [24].

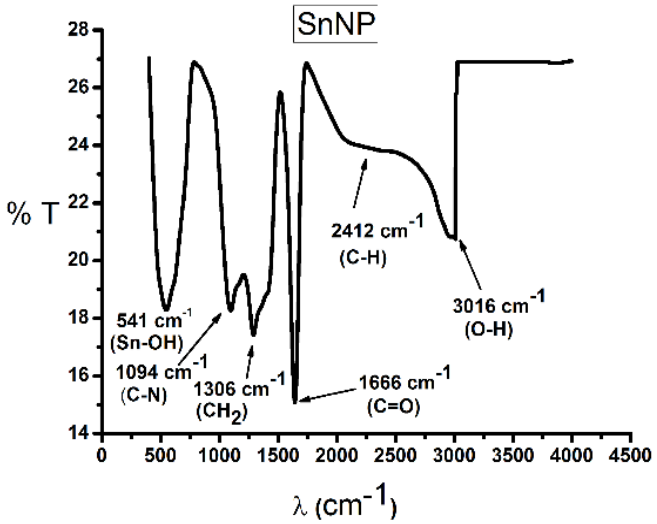

Figure 5: The FT-IR spectra of PVP capped Sn nanoparticles.

Electrochemical Application

Electrochemical response was investigated by using cyclic voltammograms of the bare GCE and modified GCEs in PBS (pH 7.0) with 25 µM BPA are shown in Figure 6. a single oxidation peak was observed for all electrodes tested in the potential window 0.3 to 0.8 V. This indicated that the oxidation reaction of BPA is a typical irreversible electrode process as reported by other authors [25]. The oxidation reaction took place on a bare GCE at +0.540 V with anodic peak current of 2.67 µA. For modified GCE the peak potential and peak current were, respectively +0.607 V and 2.35 µA for SnNP/GCE, +0.589 V and 3.87 µA for tyrosinase/GCE, +0.517 V and 3.47 µA for tyrosinase/SnNP/GCE. The oxidation peaks of tyrosinase/GCE and tyrosinase/SnNP/GCE increased significantly as compared to other electrodes. It demonstrated that tyrosinase enzyme could retain its bioactivity to a large extent when been immobilized on Sn nanoparticles by covalent binding. The oxidation current increase and the oxidation potential shift more negatively when tyrosinase and Sn nanoparticles were immobilized onto the surface of GCE [26]. This result can be attributed to the synergetic activity of tyrosinase and Sn nanoparticles, in which the negative potential shift indicates the significant electrocatalytic activity of Sn nanoparticles and tyrosinase. The mechanism of reaction of tyrosinase is due to the role of BSA acting as a stabilizing agent for the enzyme, glutaraldehyde act as a cross-linker between the GCE and the nanoparticles for the detection of BPA.

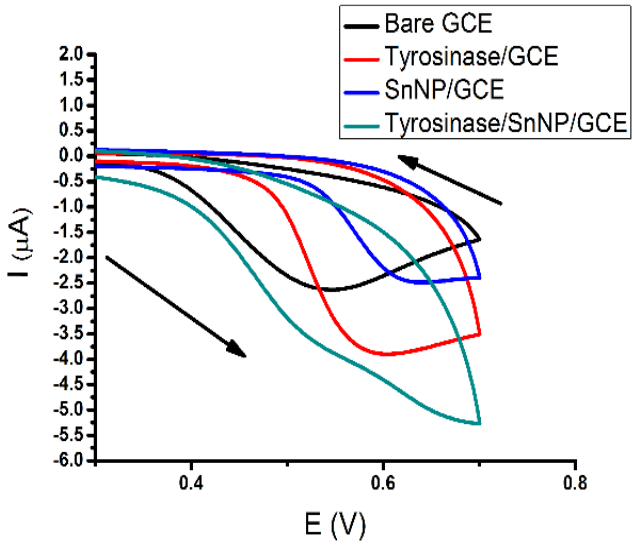

Figure 6: Cyclic voltammograms of Bare GCE, SnNP/GCE, Tyrosinase/GCE and Tyrosinase/SnNP/GCE in 0.1 M PBS (pH 7.0) containing 25 µM BPA. Scan rate: 50 mV s^{-1}. The arrow indicates scanning direction.

A typical current versus concentration plot of tyrosinase/SnNP/GCE is shown in Figure 7. Under optimum experimental conditions after successive addition of BPA, with different concentration in 0.1 M PBS (pH 7.0) under magnetic stirring. The calibration curve was linear from 0.01 to 0.10 µmol L^{-1} with a correlation coefficient of 0.989. The linear regression equation was expressed according to the function: i = 2.45 [BPA] + 1.505, where i is the resulting peak current in µA and [BPA] is the concentration of BPA in µmol L^{-1}. The Detection Limit (DL) was calculated according to the equation; $\frac{3 \times SD}{Slope}$, where SD is the standard deviation and slope of calibration curve. The DL value obtained was 1.8 nmol L^{-1} which is one of the lowest values provided by nanomaterials based on modified electrodes reported in published articles [12-14, 26]. These data verify the ability of tyrosinase/SnNP/GCE to detect BPA at nano molar levels. To verify the stability of the proposed biosensor, the response for 25 µM BPA was investigated every 6 days. Meanwhile the biosensor was stored at 4°C in PBS (pH 7.0). The electrochemical response of the biosensor was stable, retaining more than 94 % of its original response for 2 weeks and 3 days. After that, a decrease to 87 % of its original response was observed after 18 days. This good stability can be attributed to the strong binding of Sn nanoparticles and tyrosinase film with GCE.

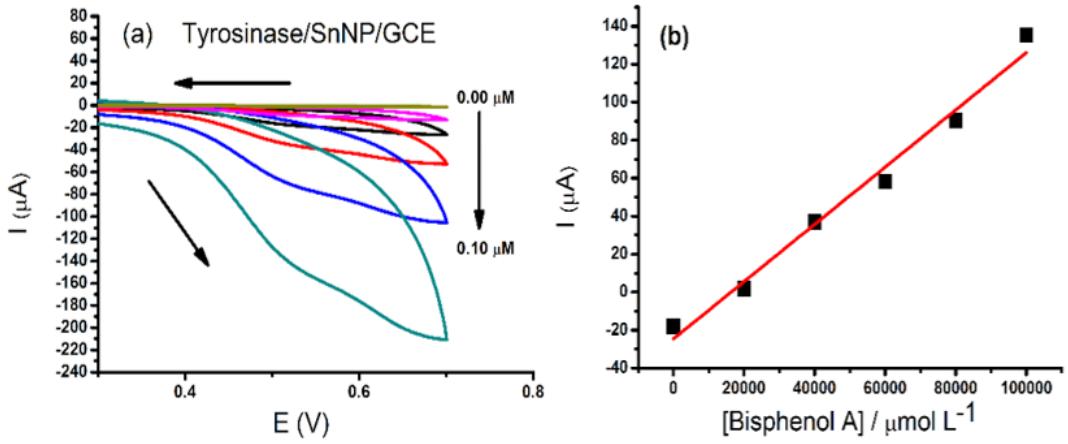

Figure 7: (a) Cyclic voltammetry for Tyrosinase/SnNP/GCE in 0.1 M PBS (pH 7.0) containing BPA (0.00, 0.02, 0.04, 0.06, 0.08, 0.10, µmol L^{-1}), Scan rate = 50.0 mV s^{-1}. **(b)** Calibration curve for BPA.

The bare and modified electrodes of tyrosinase/SnNP/GCE, tyrosinase/GCE and SnNP/GCE were characterized by Electrochemical Impedance Spectroscopy (EIS) using $[Fe(CN)_6]^{3-/4-}$ as the electrochemical redox probes. Generally, the linear part in the EIS represents the diffusion limited process while semicircle corresponds to the electron transfer limited process [25,27-29]. Figure 8 Shows Nyquist diagram of different electrodes in 0.005 M $[Fe(CN)_6]^{3-/4-}$ solution containing 0.1 M KCl. It can be observed that a large well defined semicircle was obtained at lower frequencies, corresponding to Rct = 654 Ω Bare GCE and Rct = 728 Ω SnNP/GCE, indicating strong resistance to charge transfer. When tyrosinase was deposited on the surface of GCE the impedance values obtained decreased to Rct = 516 Ω which could be attributed by enzyme electrocatalytic activity which leads to better conductivity of the electrode leading to lower interface electrical resistance. Finally, when Sn nanoparticles were drop coated together with tyrosinase on GCE [tyrosinase/SnNP/GCE] the impedance that was obtained was even more lower at Rct = 258 Ω, indicating a low charge transfer resistance. This experiment indicated a successful chemically modified GCE with Sn nanoparticles and enzyme for application for detection of BPA.

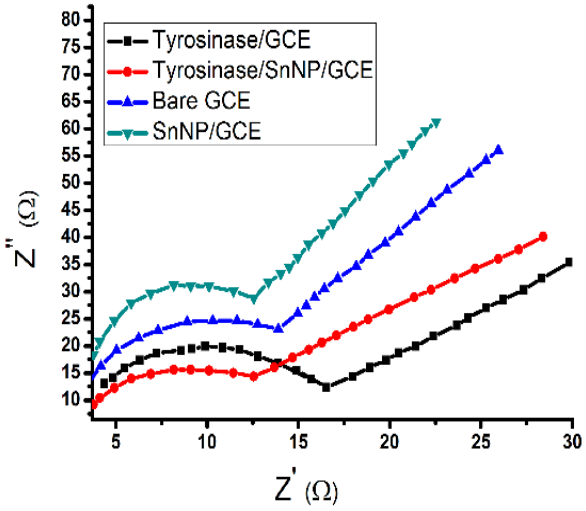

Figure 8: Nyquist plots of different electrodes in 0.1 M KCl containing 0.005 M Fe $(CN)_6]^{3-/4-}$solution for different electrodes: Bare GCE, SnNP/GCE, Tyrosinase/GCE and Tyrosinase/SnNP/GCE.

Electrochemical Impedance Spectroscopy (EIS) is a widely employed technique for the electrochemical behavior investigation of a modified electrode interface during the stepwise process [25,30]. Figure 9 shows Nyquist plots of Bare GCE, SnNP/GCE, tyrosinase/GCE and tyrosinase/SnNP/GCE in 0.1 M PBS (pH 7.0) with 25 µM BPA in a frequency range of 100 mHz -100 kHz. Impedance spectra were modelled according to the Randles equivalent circuit using analysis program with fitting error less than 2 % where Rs is the ohm resistance for the bulk electrolyte, Rct is the charge transfer resistance, Cdl is double layer capacitance and Zw is the Warburg impedance. It is obvious from the figure that modified electrode with tyrosinase/SnNP/ GCE has the lowest Rct value 219 Ω, which indicated low charge transfer. There was an increase in Rct for tyrosinase/GCE, SnNP/GCE and Bare GCE which was 316 Ω, 638 Ω and 598 Ω respectively. This indicated a strong resistance to charge transfer. The blocking of electron transfers Rct 638 Ω for SnNP/GCE is due to the excessive fouling which was improved when tyrosinase was drop coated for detection of BSA. This confirms that the enzyme was successfully immobilized on the electrode and the detection of BSA was possible.

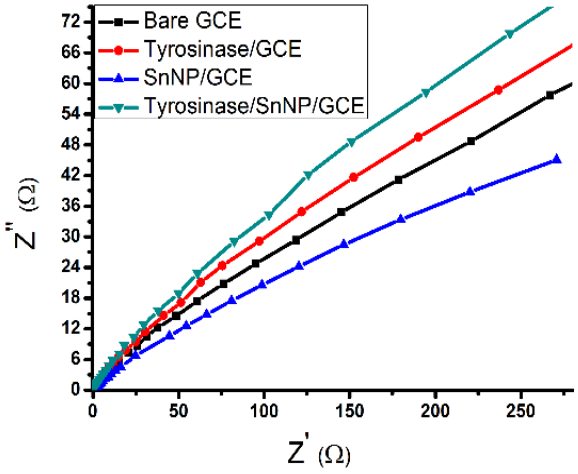

Figure 9: Nyquist plots of different electrodes in 0.1 M PBS (pH 7.0) containing 25 µM BPA solution for different electrodes: Bare GCE, SnNP/GCE, Tyrosinase/GCE and Tyrosinase/SnNP/GCE.

In Figure 10, from the bode plot it is observed at low frequency tyrosinase/SnNP/GCE have a higher total impedance as compared to tyrosinase/GCE, SnNP/GCE and Bare GCE, at higher frequencies the total impedance is more or less the same but with tyrosinase/SnNP/GCE is slightly high.

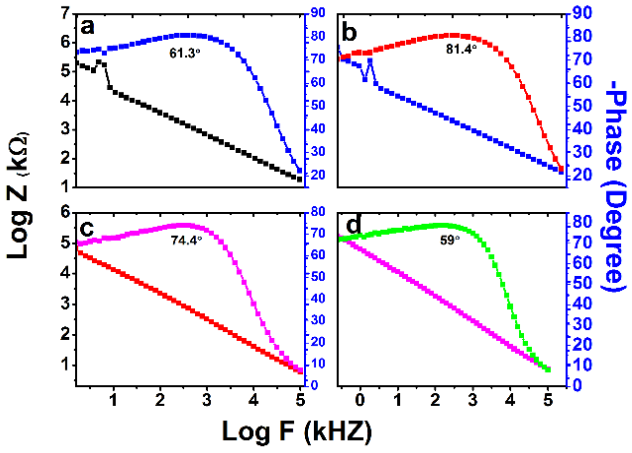

Figure 10: Bode plot for **(a)**Tyrosinase/GCE, **(b)** Tyrosinase/SnNP/GCE, **(c)** SnNP/GCE and **(d)** Bare GCE in 0.1 M PBS (pH 7.0) + 25 µM BPA and different over potentials.

Phase angle values for tyrosinase/SnNP/GCE, tyrosinase/GCE, SnNP/GCE and Bare GCE is 81°, 61°, 74° and 59° respectively, showed semiconductor behavior due to the presence of Sn nanoparticles acting as a catalyst [31-33]. It shows the presence of enzymatic reaction of tyrosinase in the system has improved conductivity significantly.

Conclusion

In this study, a novel highly sensitive and simple electrochemical detection method has been proposed for the detection of BPA in water. The present BPA sensor based on tyrosinase/SnNP/GCE gave a linear range from 0.01 to 0.10 µmol L^{-1} with a correlation coefficient of 0.989. The Detection Limit (DL) value obtained was 1.8 nmol L^{-1}, which is lowest compared to others reported in literature. Cyclic voltammetry and electrochemical impedance spectroscopy studies were very reproducible, selective and stable. The successful application of this sensor in PBS proves its effectiveness for BPA determination in water samples.

Acknowledgements

This research work was funded by South African Nuclear Human Asset and Research Programme (SANHARP), National Research Foundation (NRF), Department of Science and Technology (DST) and UNESCO-UNISA-Africa Chair in Nanoscience and Nanotechnology.

References

1. Callan AC, Hinwood AC, Heffernan A, Eaglesham G, Mueller J, et al. (2013) Urinary bisphenol A concentrations in pregnant women. Int J Hyg Environ Health 216: 641-644.
2. Ehrlich S, Williams PL, Hauser R, Missmer SA, Peretz J, et al. (2013) Urinary bisphenol A concentrations and cytochrome P450 19 A1 (Cyp19) gene expression in ovarian granulosa cells: An in vivo human study. Reprod. Toxicol 42: 18-23.
3. Jiang HM, Fang ZZ, Cao YF, Hu CM, Sun XY, et al. (2013) New insights for the risk of bisphenol A: Inhibition of UDP-Glucuronosyltransferases (UGTs). Chemosph 93: 1189-1193.
4. Longnecker MP, Harbak K, Kissling GE, Hoppin JA, Eggesbo M, et al. (2013) The concentration of bisphenol A in urine is affected by specimen collection, a preservative, and handling. Environ Res 126: 211-214.
5. Mahony JO, Moloney M, McCormack M, Nicholls IA, Mizaikoff B, et al. (2013) Design and implementation of an imprinted material for the extraction of the endocrine disruptor bisphenol A from milk. J Chromatogr B 931: 164-169.
6. Rochester JR (2013) BisphenolA and human health: A review of the literature. Reprod. Toxicol 42: 132-155.
7. Mathisen GH, Yazdani M, Rakkestad KE, Aden PK, Bodin J, et al. (2013) Prenatal exposure to bisphenol A interferes with the development of cerebellar granule neurons in mice and chicken. Int J Dev Neurosci 31: 762-769.
8. Santana, CA de Lima, JV Piovesan, A Spinelli (2017) An original ferroferric oxide and gold nanoparticles-modified glassy carbon electrode for the determination of bisphenol A, Sens. Actuators B: Chem 240: 487-496.
9. Sarigiannis ER, Karakitsios SP, Handakas E, Simou K, Solomou E, et al. (2016) Integrated exposure and risk characterization of bisphenol-A in Europe. Food and Chem Toxicol Part B 98: 134-147.
10. Ragavan KV, Rastogi NK, Thakur MS, (2013) Sensors and biosensors for analysis of bisphenol-A. Anal Chem 52: 248.
11. Wang S, Wang X, Jia B, Jing X (2017) Fabrication and characterization of poly (bisphenol A borate) with high thermal stability. Appl Surf Sci 392: 481-491.
12. Vicentini FC, Janegitz BC, Brett CMA, Fatibello-Filho O (2013) Tyrosinase biosensor based on a glassy carbon electrode modified with multi-walled carbon nanotubes and 1-butyl-3-methylimidazolium chloride within a dihexadecylphosphate film. Sens Actuators B: Chem 188: 1101-1108.
13. del Torno-de Román L, Asunción Alonso-Lomillo M, Domínguez-Renedo O, Julia Arcos-Martínez M (2016) Tyrosinase based biosensor for the electrochemical determination of sulfamethoxazole. Sens. Actuators B: Chem 227: 48-53.
14. Zehani N, Fortgang P, Lachgar MS, Baraket A, Arab M, et al. (2015) Highly sensitive electrochemical biosensor for bisphenol A detection based on a diazonium-functionalized boron-doped diamond electrode modified with a multi-walled carbon nanotube-tyrosinase hybrid film. Biosens Bioelectron 74: 830-835.
15. Guo C, Yang Q, Liang J, Wang L, Zhu Y, et al. (2016) Sn nanoparticles uniformly dispersed in N-doped hollow carbon nanospheres as anode for lithium-ion batteries. Mater Lett 184: 332.
16. Roshanghias A, Bernardi J, Ipser H (2016) An attempt to synthesize Sn-Zn-Cu alloy nanoparticles. Mater Lett 178: 10-14.
17. Vomáčka P, Štengl V, Henych J, Kormunda M (2016) Shape-controlled synthesis of Sn-doped CuO nanoparticles for catalytic degradation of Rhodamine B. J Colloid and Interface Sci 481: 28-38.
18. Wegner S, Saito M, Barthel J, Janiak C (2016) Soft wet-chemical synthesis of Ru-Sn nanoparticles from single-source ruthenocene-stannole precursors in an ionic liquid. J Organomet Chem 821: 192-196.
19. Zhang Z, Yin L (2016) Polyvinyl Pyrrolidone Wrapped Sn Nanoparticles/Carbon Xerogel Composite as Anode Material for High Performance Lithium Ion Batteries. Electrochim Acta 212: 594-602.
20. Dubey SP, Dwivedi AD, Lahtinen M, Lee C, Kwon YN, et al. (2013) Protocol for development of various plants leaves extract in single-pot synthesis of metal nanoparticles, Spectrochim. Acta Part A Mol Biomol Spectrosc 103: 134-142.
21. Xu X, Takai C, Shirai T, M Fuji (2015) Synthesis and characterization of a novel hollow nanoparticle-based SnS crystal product with microcluster-like 3D network hierarchitectures. Adv Powder Technol 26: 1327.
22. Bobadilla LF, García C, Delgado JJ, Sanz O, Romero-Sarria F, et al. (2012) Influence of PVP in magnetic properties of NiSn nanoparticles prepared by polyol method. J Magn Magn Mater 324: 4011.
23. Phelane L, Muya FN, Richards HL, Baker PGL, Iwuoha EI (2014) Polysulfone Nanocomposite Membranes with improved hydrophilicity. Electrochim. Acta 128: 326-335.
24. Chee SS, Lee JH (2014) Synthesis of sub-10-nm Sn nanoparticles from Sn(II) 2-ethylhexanoate by a modified polyol process and preparation of AgSn film by melting of the Sn nanoparticles. Thin Sol Films 562: 211-217.
25. Kochana J, Wapiennik K, Kozak J, Knihnicki P, Pollap A, et al. (2015) Tyrosinase-based biosensor for determination of bisphenolA in a flow-batch system. Talanta 144: 163-170.
26. Carralero Sanz V, Mena ML, González-Cortés A, Yáñez-Sedeño P, Pingarrón JM (2005) Development of a tyrosinase biosensor based on gold nanoparticles-modified glassy carbon electrodes: Application to the measurement of a bioelectrochemical polyphenols index in wines. Anal Chim Acta 528: 1-8.
27. Fang Y, Bullock H, Lee SA, Sekar N, Eiteman MA, et al. (2016) Detection of methyl salicylate using bi-enzyme electrochemical sensor consisting salicylate hydroxylase and tyrosinase. Biosens Bioelectron 85: 603-610.
28. Pei LZ, Cai ZY, Xie YK, Fu DG (2014) Electrochemical behaviors of benzoic acid at polyaniline/$CuGeO_3$ nanowire modified glassy carbon electrode. Measurement 24: 095701.
29. Lete C, Lupu S, Lakard B, Hihn JY, del Campo FJ (2015) Multi-analyte determination of dopamine and catechol at single-walled carbon nanotubes Conducting polymer Tyrosinase based electrochemical biosensors. J Electroanal Chem 744: 53.
30. Mita DG, Attanasio A, Arduini F, Diano N, Grano V, et al. (2007) Enzymatic determination of BPA by means of tyrosinase immobilized on different carbon carriers. Biosens Bioelectron 23: 60-65.
31. DeAngelis DA, Schulze GW, (2015) Advanced Bode Plot Techniques for Ultrasonic Transducers, Phys. Proced 63: 2-10.

32. Morgan KD, Zheng Y, Bush H, Noehren B (2016) Nyquist and Bode stability criteria to assess changes in dynamic knee stability in healthy and anterior cruciate ligament reconstructed individuals during walking. J Biomech 49: 1686-1891.

33. Berce P, Skale S, Slemnik M (2015) Electrochemical impedance spectroscopy study of waterborne coatings film formation. Prog Org Coat 82: 1-6.